Investigation of the PEGASES thruster magnetic filter via laser photodetachment experiments

IEPC-2015-380／ISTS-2015-b-380

Presented at Joint Conference of 30th International Symposium on Space Technology and Science, 34th International Electric Propulsion Conference and 6th Nano-satellite Symposium Hyogo-Kobe, Japan July 4–10, 2015

D. Renaud* and S. Mazouffre†

ICARE - CNRS, 1C Avenue de la Recherche Scientifique, 45071 Orleans, France

E. Pawelec

University of Opole, Oleska 48, Opole, Poland

PEGASES is an unconventional gridded ion engine concept for which the discharge is created in a strongly electronegative gas. The electronegative plasma is transformed into an electron-free plasma, i.e. an ion-ion plasma, using a magnetic filter to trap electrons. Electron collisions with heavy particles result in a drop in electron temperature, allowing cold electrons to attach to molecules to form negative ions. PhotoDetachment (LPD) experiments have been carried out in the magnetic barrier of the device. A 266 nm pulsed laser beam is used to detach electrons and an electrostatic probe is used to measure the resulting electron current. The impact of the magnetic field strength, the gas pressure and the input RF power on the negative ion production and transport have been studied. The experiments reveal electronegativities exceeding 10, negative ion densities exceeding 10^{16}m^{-3}, as well as an anisotropy of the plasma due to a magnetic field induced electron drift.

Nomenclature

α	= electronegativity	β	= current ratio
σ	= cross section of photodetachment	$h\nu$	= photon energy
ΔI	= LPD current	Δn_e	= electron density from LPD
Δn^-	= negative ions density from LPD	B	= magnetic field
e	= elementary charge	E	= electric field
$I^{-,+}$	= negative or positive ions current	I_{dc}	= plasma Current
I_e	= electron current	J_{ed}	= electron drift current
j	= current density	P	= laser power
n^-	= negative ions density	n_e	= electron density
S	= probe collection area	S_L	= spot area
v_e	= electron velocity	v_d	= drift velocity

*Ph.D. student, Electric Propulsion Team, denis.renaud@cnrs-orleans.fr

†Research Scientist, Electric Propulsion Team Leader, stephane.mazouffre@cnrs-orleans.fr

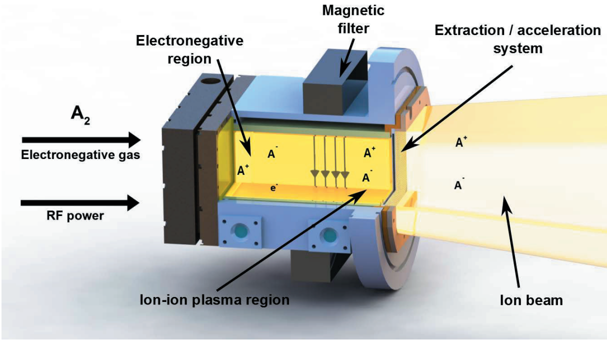

Figure 1. 3D view of PEGASES

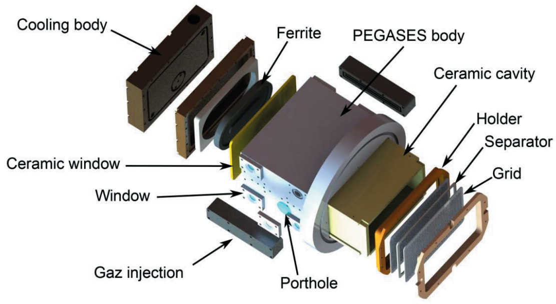

Figure 2. Exploded-view drawing of PEGASES

I. Introduction: the PEGASES ion source

The PEGASES - standing for Plasma propulsion with Electronegative GASES - is a thruster based on an unconventional gridded ion source concept for which the discharge is created in a strongly electronegative gas.[1–5] The PEGASES operation is explained in figure 1. Contrary to classical gridded thrusters, which only accelerate positive ions, PEGASES ejects positive and negative ions. The ionization stage of PEGASES can be divided into two main parts. Firstly, an inductively-coupled RF discharge is ignited inside a rectangular dielectric cavity with an electronegative gas such as sulfur hexafluoride (SF_6). This operation generates an electronegative plasma mainly composed of electrons and positive ions. Some negative ions also appear in low quantity as well as molecular fragments due to dissociative reactions. Secondly, two magnets are fixed on the thruster sides to enable the confinement of electrons, which results into an ion-ion plasma.[6] In addition electrons trapped in the strong magnetic field region are rapidly cooled down due to the collision with neutral heavy particles.[4] An increase in the production of negative ions occurs by attachment of cold electrons with neutrals. In the region of ion-ion plasma, alternate polarization[7] is utilized on the screen grid in order to extract positive and negative ions. The two ion beams exhausted by alternating acceleration recombine to form a beam with a low charge density due to the efficient recombination between positive and negative ions. The acceleration grid is kept at ground. Because of their high mobility, electrons do not allow to efficiently extract negative ions. It is therefore essential that electrons are well trapped. The magnetic filter is therefore a critical component of the PEGASES engine. As an innovative thruster, PEGASES presents several advantages compared to conventional thrusters. Interaction with the spacecraft is reduced thanks to the quick neutralization through ion-ion collisions, thereby rendering the cathode for neutralization useless. Moreover, a promising propellant for PEGASES is Iodine (I_2), a strongly electronegative gas, which can be easily stored in solid state under space flight conditions.[8] The propellant storage volume is then strongly reduced, an important challenge for any space vehicle.

An exploded-view drawing of PEGASES is represented in figure 2. The discharge is produced inside a BN-SiO_2 cavity with a section of 6 cm by 10 cm and 12 cm in length. The input RF power ranges from 80 to 250 W. It is generated by a planar antenna embedded into a ferrite shield which is water-cooled. The RF wave oscillates at 4.2 MHz. The ferrite shield permits to increase the energy transfer to the plasma discharge in such away a purely inductive coupling is achieved. Due to an alumina plate which covers the antenna to protect it, cavity is floating. The thruster's two sides are perforated with 8 holes permitting the gas injection. Either electronegative gases or noble gases are injected. The latter are used for comparison with conventional ion engines. Permanent neodymium magnets are fixed perpendicularly to the injection sections and they are used to generate the transverse magnetic field of the filter. The magnitude of the field can be varied from 0 to 340 G according to the number of magnet bars. Two grids are placed inside a PEEK holder with a 2 mm thick separator in ceramic. The two planar grids are made of stainless steel. The hole size is 2 mm. The grids thickness is 0.8 mm and the transparency is 60 %.

II. The photo-detachment diagnostic techniques

The Laser PhotoDetachment (LPD) is a non-intrusive technique that allows to detect negative ions A^- and to assess the local plasma electronegativity and the negative ion absolute number density.[9] The principle behind the LPD technique is relatively straightforward. When a negative ion is illuminated with a laser beam, the electron is removed, i.e. detached, if the photon energy is above the binding energy, the so-called electron affinity. The LPD can be summarized through the following equation:

$$A^- + h\nu \longrightarrow A + e^-, \tag{1}$$

where A is a neutral atom and e an electron. LPD therefore transforms the negative ion density into an electron density. The latter can easily be determined by means of a Langmuir probe, a Hairpin probe or microwave interferometry.[10,11]

The ratio of the LPD electron current to the electron current in steady state gives an information about the electronegativity, α:

$$\frac{\Delta I}{I_{dc}} = \frac{\Delta j_{e,lpd} S_{lpd}}{j_{e,dc} S_{dc}} = \frac{e \Delta n_{e,lpd} v_{e,lpd} S_{lpd}}{e n_{e,dc} v_{e,dc} S_{dc}} \approx \frac{\Delta n_e}{n_e} = \frac{n_-}{n_e} = \alpha, \tag{2}$$

where j is a current density, S the probe collection area, v the electron velocity and n the density. The subscript e and $-$ refers to electron and negative ion, respectively. The subscript *lpd*, respectively *dc*, refers to the value obtained during the laser photodetachment, respectively in steady state. The symbol Δ indicates a sudden change in the electron current due to the laser pulse. In order to link the photodetachment signal to the plasma electronegativity α, several assumptions are necessary, as can be seen in Eq. 4. Indeed, the electron velocity, or the EEDF, and the collection area are assumed to be identical in steady state and during the LPD. Besides, the measured DC current is only due to electron in this analysis, neglecting the negative ion contribution. Such assumptions may be valid when α is small (< 1), i.e. when the plasma is weakly electronegative. However, when the plasma is highly electronegative, or ion-ion, i.e. electron free, previous equation is not valid anymore due to the change in the plasma and sheath dynamics driven by the laser pulse effect.

In the remainder of this paper, we will use a parameter termed β, which is defined as

$$\beta = \frac{\Delta I}{I_{dc}} = \frac{\Delta I}{I_e + I_-}, \tag{3}$$

The β coefficient is just the ratio of the two currents with and without laser illumination but it does not correspond to the electronegativity. Previous assumptions do not hold. Moreover, the investigated plasma discharge is strongly electronegative ($\beta \gg 1$) and the saturation current measured by the Langmuir probe at a high positive voltage is in fact mostly due to the negative ions. The electron contribution is difficult to isolate and no attempt was made in this work. Therefore, β can be seen as the lower limit of α.
The choice of the laser wavelength is related to the negative ion species present in the plasma. The photon energy must be larger to the electron affinity of the negative ion. The fraction of detached electron depends on the laser wavelength. The theoretical fraction is described by:

$$\frac{\Delta n_-}{n_-} = 1 - exp\left(-\frac{\sigma P}{h\nu S_L}\right), \tag{4}$$

where σ is the photodetachment cross section of negative ion and P/S the laser power density. The laser must provide a high power in order to detach all negative ions. This technique can measure the density of negative ions without disturbing the plasma medium. In addition, the velocity can be obtained[12] by using two consecutive laser pulses.

III. Experimental setup

A. Optical bench

Figure 3 shows the optical bench for laser photo-detachment in SF_6 plasma. The laser beam wavelength is chosen as a function of the electron affinity of molecular fragments present in SF_6 plasma. The electron affinity of SF_5^- is the highest. The electron affinity ranges between 3.8 eV[13] and 4.2 eV.[14] The laser is a

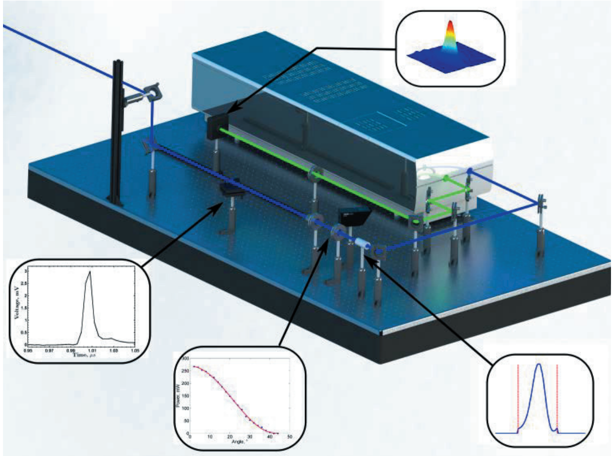

Figure 3. Optical bench for laser photodetachment inside the PEGASES thruster.

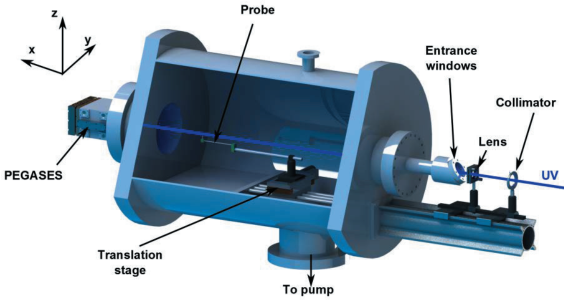

Figure 4. Vacuum tank with Langmuir probe mounted on the translation stage and the laser beam.

Nd-YAG at 1064 nm with a frequency of 10 Hz from Quanta-Ray. Two crystals for 2nd harmonic generation allow to have a wavelength of 266 nm, i.e. 4.65 eV, to detach all fragments. The beam is directed by four high fluence 266 nm dielectric mirrors inside the PEGASES cavity. A aluminium collimator with a length of 50 mm and a diameter of 7 mm allow to cut the wings of the laser beam profile. The laser power is adjusted by two optics: a polariser which change the polarization of laser beam and a Glan prism that transmits only one polarization component. The power can be varied between 0 and 28 mJ per pulse by changing the laser polarization. In addition, a wedge prism is used to split the beam in two parts. The main beam is sent to the PEGASES discharge. A secondary, low intensity UV beam, is directed towards a fast photodiode to monitor the pulse temporal profile. The pulse duration (FWHM) is 8 ns. Notice the signal from the photodiode also serves as a time reference for LPD measurements. Finally the beam spatial profile is measured with a residual green beam at 532 nm behind the first second harmonic generation stage. A small CCD camera is used to capture the light distribution. The beam profile is almost Gaussian with a full-width at half-maximum of 8 mm. The UV beam is assumed to exhibit the same features.

B. Detection system

The PEGASES thruster is mounted on the the EPIC test chamber. EPIC is a stainless-steel cylindrical tank with a diameter of 56 cm and a length of 82 cm. It is equipped with various optical windows, access ports and electrical vacuum feedthroughs. The tank is evacuated by a 1000 l/s in N_2 turbomolecular pump connected to a 65 m^3/h primary pump. The residual pressure with no gas injection is 2.10^{-6} mbar. The background pressure reaches typically 5.10^{-4} mbar when PEGASES is fired. Figure 4 shows the EPIC chamber with the thruster. As can be seen in Figure 4, the laser beam is shined through a tilted UV quartz window along the chamber centerline. A 1500 mm focal length UV lens is used to focus the laser beam in such a way the spot size at the measurement location is 2 mm. In order to detect electron from photo-detachment a Langmuir probe is used. The probe has a L-shape for three reasons: to limit the probe sputtering at hight fluence, to be perpendicular to the magnetic field lines and to be entirely covered by the laser beam. The probe consist of a ceramic tube (Alumina or quartz) with inside a platinum wire with a length of 3 mm and a diameter of 200 μm. The properties of platinum allows to diminish the sputtering effect and the chemical reaction with the SF_6. Moreover, this probe is mounted on a translation stage to move in x and y directions. The probe voltage is chosen above the plasma potential to reach the saturation regime. However, in the case of high electron density the signal can be disturbed by thermo-emission effect. This effect will be discussed in section C. The Langmuir probe is connected to a RC circuit to detect the variation of current from photo-detachment, see fig 5. The circuit allows to vary the resistance connected to the probe to increase or decrease the resolution. The signal is collected an oscilloscope with a 50 Ω impedance. The circuit was designed following advice given in the literature.[12,15] The values for R1 is 47 Ω , R2 is 100 Ω, R3 is 4.7 kΩ and C is 1.08 μF. To obtain the electron DC current, the I-V characteristic curve of the probe is acquired either with the ALP system from Impedans or directly with a sourcemeter (Keithley 2410).

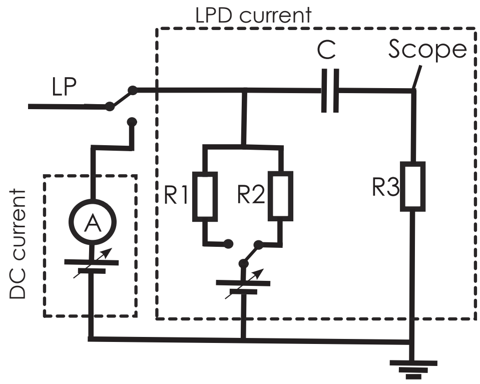

Figure 5. Electrical circuit connected to the Langmuir probe to measure the current form laser photo-detachment

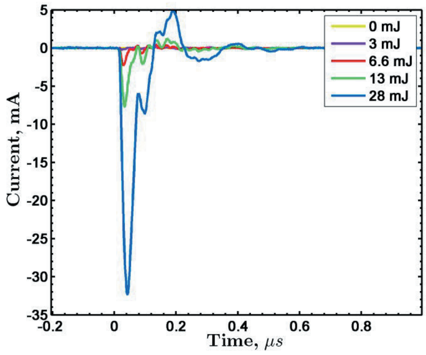

Figure 6. Photo-emission effect measured with the probe biased at +50 V in a mixture of 50% SF_6 + 50% Kr with 10 sccm (160 W RF power, 125 G).

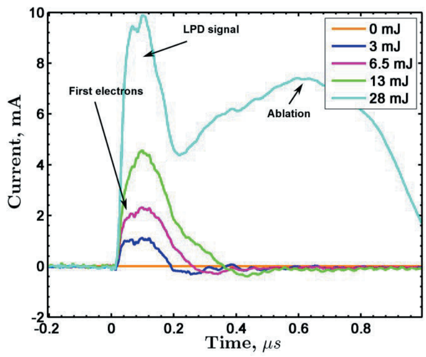

Figure 7. Ablation effect with a probe bias of -50 V (50% SF_6 + 50% Kr, 10 sccm, 160 W RF power, 125 G).

C. Preliminary measurements

Some materials are destroyed with a high laser fluence with a wavelength of 266 nm. Then, the ablation of the cavity walls and the probe ceramic tube must be investigated. The sputtering effect has been seen in the literature with both Langmuir and hairpin probe and it can lead to overestimate the LPD signal.[11,16] Several materials have been tested for the probe construction: Pt and W for the tip and alumina and quartz for the insulator. The final design was a Pt wire inserted into an alumina tube.

Figure 6 shows the signal collected by a -50 V bias probe in a mixture of 50% SF_6 + 50% Kr with a total gas flux of 10 sccm. The input RF power is 160 W and the magnetic field magnitude is 125 G. The negative signal corresponds either to collection of positive ion or to electron emission. However, the signal depends on the laser power and is very short, its duration being around a few tens of ns. These characteristics correspond to electron emission under photon bombardment.

Figure 7 shows the signal collected by a +50 V bias probe in a mixture of 50% SF_6 + 50% Kr with 10 sccm, 160 W imput RF power and 125 G. When the probe is positively biased, the collected current is positive in comparison with the negative bias case. The current is therefore composed of electrons. Three peaks can be distinguished in the current traces in Fig. 7. The first and narrow peak after the laser pulse (see also Fig. 9) is the signature of electrons detached in the sheath of the Langmuir probe.[12] The second and strongest peak is said to be the LPD signal. The two peaks are always present but their magnitude depends on the laser beam energy. On the contrary, the third peak only appears above a certain laser energy threshold. The third peak duration is typically 1 μs; It is much longer than the duration of the first two phenomena. The third peak therefore corresponds to the ablation of the probe material.

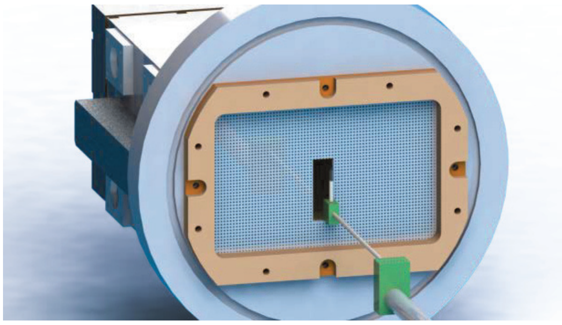

Figure 8. Front view of a PEGASES CAD model with a rectangular hole and a L-shaped Langmuir probe.

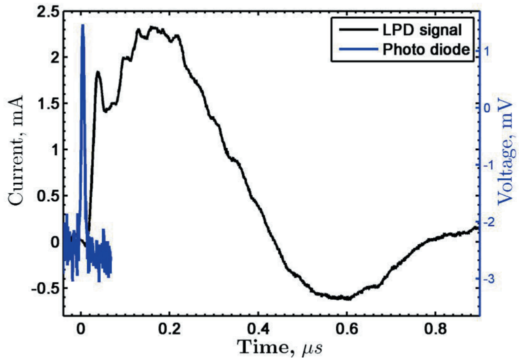

Figure 9. LPD signal in 5 sccm SF6 + 5 sccm Kr, 160 W imput RF power and a magnetic field of 125 G. The blue trace corresponds to the laser temporal evolution measured by a photo-diode.

IV. Measurements through the magnetic barrier

A. LPD signal

A screen is used inside the PEGASES cavity to protect the cavity back ceramic from laser ablation. The screen is an electrically-floating rectangular copper plate (dimensions 50×22×4 mm). While coppper offers good resistance to UV bombardment,[17] it also reacts with sulfur; this may modify the plasma composition to some degree.

A rectangular hole (10×30 mm) was made through the grids of PEGASES to allow probe motion inside the cavity, as seen in Fig. 8. A mixture of Kr and SF_6 is used to guarantee the stabilization of the plasma. The power transfer efficiency (PTE[18]) is used to quantify the plasma stability; a stable discharge corresponds to a high PTE, found for example in a Kr plasma. The high PTE of a Kr plasma is due to the low ionization energy of the gas, which allows sufficient quantities of electrons to be produced to maintain the discharge. The PTE of the SF_6 plasma is lower as the RF power can be dissipated into dissociation of the SF_6 into several molecular fragments. A mixture of 50% SF_6 + 50% Kr has been chosen with the maximum flow rate of 10 sccm to maintain plasma stability. As we will see shortly, such a mixture also generates a large number of negative ions.

Figure 9 shows a typical LPD trace (black line) acquired with our laser system inside the PEGASES cavity. There are two peaks of positive current. The first electrons are collected after the laser shot inside the sheath and correspond to the narrower peak. The maximum amplitude of the LPD signal corresponds to the LPD current Δ I. The negative peak appears once ions have diffused across the photodetachment area.

The negative ion temperature can be estimated using the ion velocity. A temperature of around 0.1 eV and 0.9 eV has been determined using F^- and SF_6^- ions and the value of the beam diameter.[12] The negative ion temperatures are higher than the 400 K of the positive ions. Their high temperatures are due to the dissociation energy gained during electron attachment on the neutrals. The blue trace corresponds to the laser temporal evolution measured by photo-diode.

Figure 10 shows the signal generated by screen ablation as a function of probe position. The first positive peak represents signal collected by laser photodetachment and the second broader peak is due to electrons generated from copper ablation. The measurements were performed under the same conditions as Fig. 9. The measurements are limited by the position of the copper screen; the ablation signal can mask the LPD signal close to the antenna (x = 0 cm). Moreover, a screen inside a plasma produces a wake effect and modifies the plasma dynamics.

The laser power must be chosen as a function of the parasitic effects and the ratio Δ I / I_{dc}, to guarantee the optimization of LPD signal. Figure 11 represents the current ratio as a function of laser fluence. The plasma parameters are: 5 sccm SF6 + 5 sccm Kr, 150 W imput RF power and 257 G. The negative ions are not all detached until 0.4 J.cm^{-2}, due to the low fluence. The curve begins to saturate after this threshold, however, the probe ablation already starts at 0.5 J.cm^{-2}. The working fluence in these experiments is between 0.4 and 0.5 J.cm^{-2}. The curve shown is fitted by Eq. 4. The negative ion cross section extracted from this

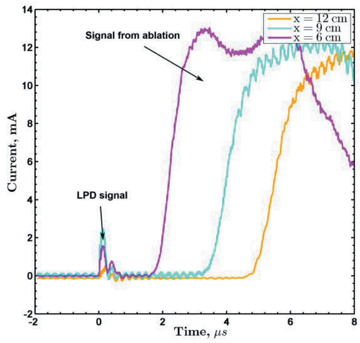

Figure 10. Signal generated by screen ablation as a function of probe position.

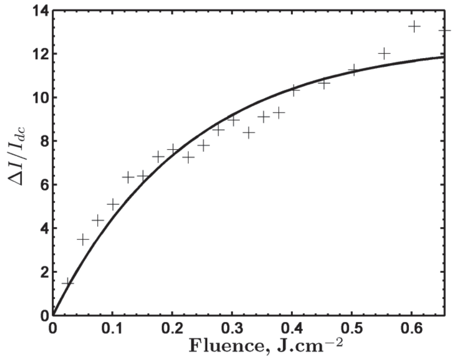

Figure 11. Collected current against laser fluence. The plasma parameters are 5 sccm SF6 + 5 sccm Kr, 150 W RF power and 257 G.

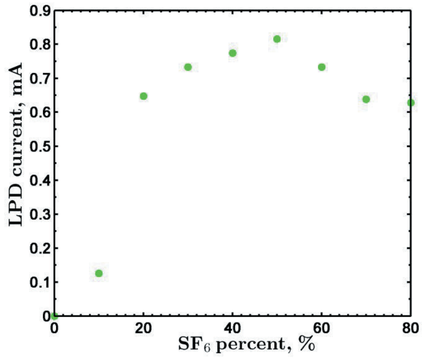

Figure 12. LPD current as a function of SF_6 percentage in an SF_6-Kr mixture for 10 sccm and 120 G.

fit is close to that of fluorine; the data gives $4.1.10^{-18}$ m^{-2}, comparable to the standard value[19] of 6.10^{-18} m^{-2} found in the literature.[20] These measurements do not permit conclusions to be drawn concerning the plasma composition, and must be coupled with another diagnostic for this to be possible. The laser can modify the composition locally by photo-dissociation; for instance, the $SF6^-$ ions can be transformed into F^- by the reaction:

$$SF_6^- + h\nu \longrightarrow SF^- + SF_5$$
$$SF^- + h\nu \longrightarrow F^- + S$$
$$F^- + h\nu \longrightarrow F + e^-$$

However, the detected negative ion density does not change.

Figure 12 illustrates the LPD amplitude as a function of the percentage of SF_6 in an SF_6-Kr mixture, for 10 sccm and 120 G. The LPD current is low between 10 and 20 % due to the mixture being primarily composed of Kr and the low proportion of negative ions present. This current increases with the proportion of SF_6 to a maximum value at 50 % in accordance with an SF_6-Ar mixture.[21] Afterwards, for higher proportions of SF_6 (between 60 and 80 %), the positive and negative ion populations diminish due to the low ionization rate.

B. Distribution of β and LPD current

Figure 13 a) represents the β measurements through of the PEGASES cavity as a function of the magnetic field. The plasma parameters are: $5sccmSF6 + 5sccmKr$, 150 W imput RF power. The magnets were placed at 7.5 cm of the antenna. The grids are at 12 cm. The β factor increases only in the strong field

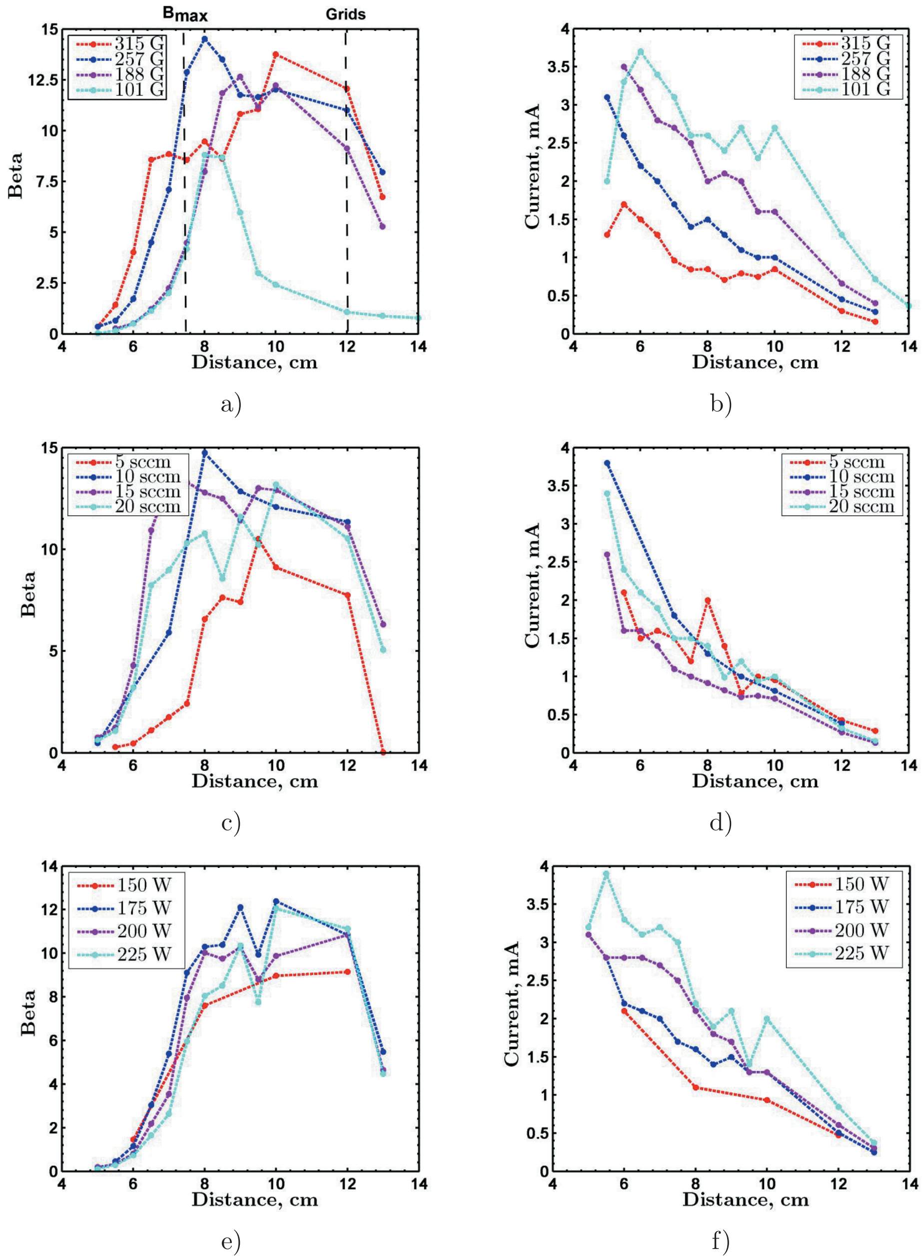

Figure 13. LPD measurements inside the PEGASES thruster: Beta (left) and current from negative ions (right). The position x = 12 refers to the exit plane. Plots a) and b) show the magnetic field effect. Plots c) and d) illustrate the flux effect. Images e) and f) represent the power effect. Measurements were performed with a SF_6 / Kr mixture (150 W RF power, 5 sccm SF6 + 5 sccm Kr, 188 G).

area. The maximum is reached beyond the magnets position. There is an effect of the magnetic field on the production of negative ions or on the electron filtering. However, the increase of the magnetic field strength shows a limit of the β maximum. The β factor decreases beyond the grids but at low B-field. In that case β follows the magnetic field profile. This effect can be linked to the diminution of the electron current from negative ions shown in figures 13 b), d) and f).

The LPD current diminishes as a function of the magnetic field strength. Several mechanisms can explain the diminution of the current along the x direction: recombination effect between pairs of positive and negative ions, losses due to collision events, expansion of the flow and magnetic confinement of light ions. Moreover, the Rf power coupling is disturbed by the magnetic field and it diminishes with the magnetic

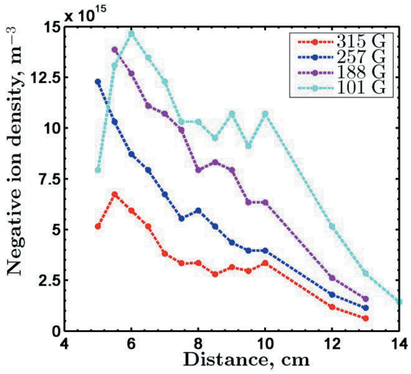

Figure 14. Estimation of negative ion density as function of magnetic field.

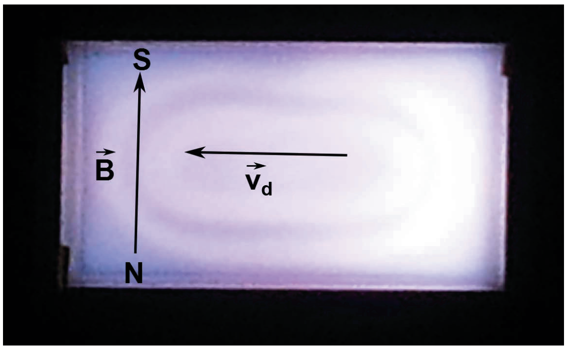

Figure 15. Front view of PEGASES without grids with 10 sccm of SF_6, 190 W and 190 G (polarization SN)

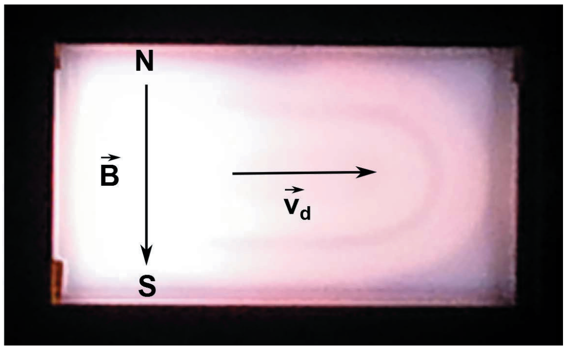

Figure 16. Front view of PEGASES without grids with 10 sccm of SF_6, 190 W and 190 G (polarization NS)

field strength. Figure 13 c) represents the β with the gas flow rate for a 50 % mixture. The Beta coefficient is around 8 at low gas flow i.e. at low pressure. There is no evolution beyond this 5 sccm due to low electron current. Figure 13 e) illustrates the measurements as a function of the RF power. The Beta is not much influenced by the RF power contrary to the current, see Fig. 13 f). The observed increase in LPD current with the RF power may be a sign for an increase in the negative ion density. The grid assembly location is critical for ensuring a large current. In fact, the LPD current decreases whatever the parameters. The RF power must be higher and the pressure must be around 10 sccm in order to guarantee a high negative ion current.

The current from LPD measurements permits an estimation of the negative ion density. The density is estimated using certain assumptions. The area collection for the LPD measurement is assumed to be the probe surface and the electron energy is taken to be $E_{LPD} = h\nu$ - EA, where EA is an electron affinity. The photodetachment current collected by the Langmuir probe is between 1 and 3 mA. The density is approximately 10^{16} m^{-3}, determined using the electron affinity of fluorine, EA(F^-) = 3.4 eV. Figure 14 shows an estimation of negative ion density as a function of magnetic field strength. The previous measurements with Langmuir probe calculation shows a negative ion density of 10^{18} m^{-3}.[4] This difference can be due to the hypothesis of electron velocity or the collection surface.

V. Asymmetry of the plasma

A. Light distribution

Magnetized plasma discharge can generate unstable structures.[22,23] As demonstrated in the works of D. Gerst and J. Bredin,[24,25] PEGASES exhibits plasma inhomogeneities due to the existence of the magnetic barrier.

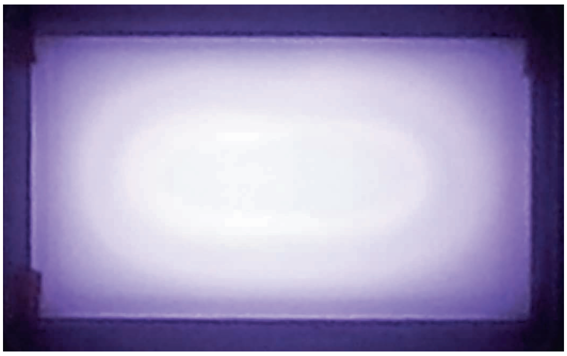

Figure 17. Front view of the PEGASES thruster without grids with 10 sccm of xenon, 150 W input power and without magnetic field.

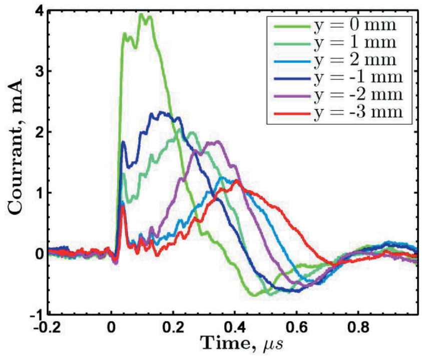

Figure 18. LPD signal collected by the probe as a function of the distance to the laser beam. The plasma parameters were 5 sccm SF6 + 5 sccm Kr, 160 W, 125 G. Grids were removed (open cavity).

Figure 15 and 16 are a front view photograph of the PEGASES cavity. The thruster is operated with 10 sccm of SF_6, 190 W and magnets are mounted with SN configuration for the picture on the left (the south pole is on the top of the figure) and NS for the picture on the right (the north pole is on the top of the figure). The magnetic field strength is 190 G. The plasma brightness is strongly inhomogeneous and asymmetrical. Depending on the direction of the magnetic field, the plasma is concentrated either on the left side (SN configuration) or on the right side (NS configuration) of the cavity. The asymmetry is present with other gases like Xe, Kr, Ar. Figure 17 shows a front view of the PEGASES thruster without grids with 10 sccm of xenon, 150 W input power and without magnetic field. In that case the light distribution is perfectly homogeneous, which indicates the observed inhomogeneity is due to the magnetic field and not to the RF coil or an asymmetrical gas flow injection.

B. LPD measurements

Figure 18 shows the LPD current traces as a function of the Langmuir probe position in the y direction. The UV laser is kept fixed along the axis of the PEGASES cavity. Its position is here refereed to as y = 0 mm. The amplitude and temporal positions depend clearly on the probe position. In fact, the collection surface depend on the distance between the probe and the laser center. The temporal position of the peaks can be used to calculate the velocity of the disturbance. Figure 19 shows the time of arrival of LPD peaks. The time delay depends linearly on the distance. The curve exhibits a V-shape. Interestingly, it is not symmetrical with respect to the laser axis. The trend changes according to the magnet polarization. The slope for each branch of V-curve gives directly the velocity of the propagating electrons. Table 1 shows the velocity. The velocity is relatively low, around a few km/s. It does not correspond to a typical electron velocity unless the latters are extremely cold. The electron collected by the probe must diffuse with the ions. The measured velocities are between 4.7 and 22.9 km/s; It could reflects the ambipolar diffusion of the charged particles in a complex plasma with electrons, positive and negative ions. The higher velocities for SN config., respectively NS config., correspond to the positive slope, respectively negative slope. The v-curve become symmetrical without magnetic field (see fig. 20). The asymmetry observed with the V-curve are of course connected to the plasma inhomogeneity previously described.

This structure can be explained by a drift in the magnetized plasma. We may consider a fluid model for the electrons and neglect the ions, which are essentially unmagnetized. The electron drift current $\mathbf{J}_e$ can be written as:

$$\mathbf{J}_{ed} = -en_e\mathbf{v}_d, \tag{5}$$

where e is the electron charge, n_e the electron density and $\mathbf{v}_d$ the drift velocity described by:

$$\mathbf{v}_d = \frac{\mathbf{E}\times\mathbf{B}}{B^2} + \frac{\bigtriangledown p\times\mathbf{B}}{en_eB^2}, \tag{6}$$

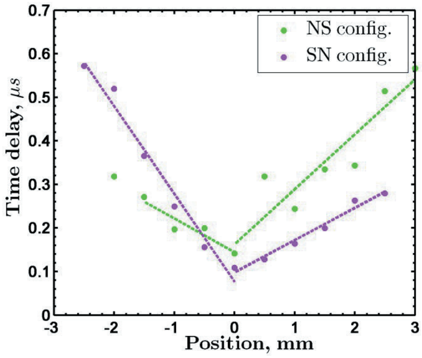

Figure 19. The V-curve measurements at x = 10 cm for two magnetic polarisations: S-N and N-S. The plasma parameters were 5 sccm SF6 + 5 sccm Kr, 150 W, 188 G (open cavity).

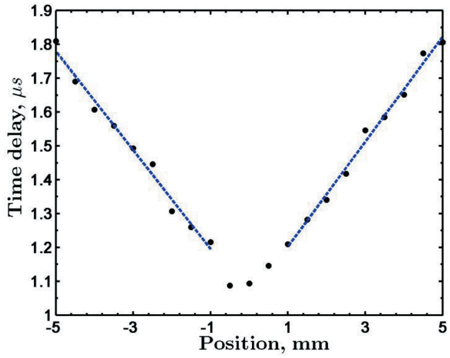

Figure 20. The V-curve measurements at x = 12 cm without magnetic field. The plasma parameters were 5 sccm SF6 + 5 sccm Kr, 160 W (open cavity).

	V-curve velocity, km/s			
	SN config.		NS config.	
	negative slope	positive slope	negative slope	positive slope
x = 12 cm	7.3	8.9	22.9	10.1
x = 10 cm	4.9	13.5	12.9	7.9
x = 8 cm	4.7	14.6	8.7	4.7
x = 6 cm	6.8	7.7		

Table 1. Velocity from LPD measurements.

The drift velocity can be divided into two components: the $\mathbf{E} \times \mathbf{B}$ drift and the diamagnetic drift. The first part of the equation has an important contribution to the drift. This equation determines the electron flux to the wall on the right, respectively left, for the SN configuration, respectively the NS configuration, as seen in Figs. 15 and 16.

C. Symmetry factor

The Langmuir probe offers the possibility to measure the magnetic effect along the PEGASES cavity in a SF_6 plasma. A symmetry factor (SF) is defined as the ratio of saturation current of positive ions and negative charge:

$$SF = \frac{I^+}{I^- + I_e}, \tag{7}$$

This ratio depend essentially on the contribution of the electron current. The ratio tends to 0 in the case of an electropositive plasma. The ratio is 1 in the case of a symmetrical ion-ion plasma i.e. when positive and negative ions have the same mass and the same temperature. Figure 21 illustrates the measurements of SF inside the cavity of PEGASES at x = 12 cm along the y-direction. The plasma parameters were 5 sccm SF6 + 5 sccm Kr, 150 W, 188 G. The cavity was open (no grid assembly). The SN configuration is represented by circles and the NS configuration by triangles. The SF is not symmetrical along the y-direction with respect to the thruster axis whatever the B-field strength. A low SF factor indicates an important contribution of the electron current. This plot shows the asymmetry of plasma along y due to the electron drift. The trend of the SF factor is in perfect agreement with the preceding pictures of the light distribution.

VI. Conclusion

LPD measurements have been performed inside the PEGASES cavity. The impact of the magnetic field strength, the gas pressure and the input RF power on negative ion production and transport have been stud-

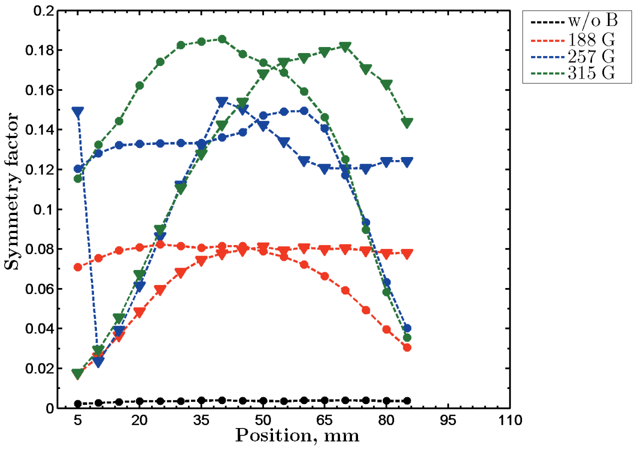

Figure 21. Symmetry factor as a function of the magnetic field. The SN configuration is represented by circles and the NS configuration by triangles. The plasma parameters were 5 sccm SF6 + 5 sccm Kr, 150 W, 188 G and the cavity was open (no grids).

ied. Measurements reveal an electronegativity above 10. An accurate determination of the electronegativity, however, requires measurements via another technique.

An examination of the magnetic field in the thruster cavity, via imaging and LPD measurements, reveals plasma asymmetry. Magnetic fields above 100 G push electrons towards the cavity walls. The electronegativity must be increased to reduce the electron density and the plasma asymmetry; this will permit the uniform extraction of negative ions and facilitate optimization of the ion source. In future work, the beam properties will be studied by LPD measurements using alternate voltage.

Acknowledgments

This research was financially supported by the ANR under grant ANR-11-BS09-040. Denis Renaud benefits from a Ph.D. grant from AIRBUS DS - R&T - Innovative Electrical Propulsion project. The authors would like to thank Ane Aanesland for useful discussions and advices.

References

[1]A. Aanesland, A. Meige and P. Chabert. Electric propulsion using ion-ion plasmas. *J. Phys.: Conf. Ser.*, 162:012009, 2009.

[2]A. Aanesland, S. Mazouffre and P. Chabert. Pegases a new promising electric propulsion concept. *europhysicsnews*, 42:28, 2011.

[3]A. Aanesland, J. Bredin, P. Chabert, and V. Godyak. Electron energy distribution function and plasma parameters across magnetic filters. *Appl. Phys. Lett.*, 100:044102, 2012.

[4]Bredin J., Chabert P. and Aanesland A. Langmuir probe analysis of highly electronegative plasmas. *Appl. Phys. Lett.*, 102:154107, 2013.

[5]D. Rafalskyi, L. Popelier, and A. Aanesland. Experimental validation of the dual positive and negative ion beam acceleration in the plasma propulsion with electronegative gases thruster. *J. Appl. Phys.*, 115:053301, 2014.

[6]D. J. Economou. Fundamentals and applications of ion-ion plasmas. *Applied Surface Science*, 253:6672, 2007.

[7]T. Lafleur, D. Rafalskyi and A. Aanesland. Alternate extraction and acceleration of positive and negative ions from a gridded plasma source. *Plasma Sources Sci. Technol.*, 24:015005, 2014.

[8]J. Szabo, M. Robin, S. Paintal, B. Pote, V. Hruby, C. Freeman. Iodine propellant space propulsion. In *33rd International Electric Propulsion Conference, Washington, D.C., IEPC-2013-311*, 2013.

[9]P.G. Datskos, J.G. Carter, L.G. Christophorou. Photodetachment of SF_6^-. *Chemical Physics Letters*, 239:38–43, 1995.

[10]C. Kullig, K. Dittmann and J. Meichsner. Analysis of negative ions in a cc-rf oxygen plasma by means of laser photodetachment and microwave interferometry. In *30th ICPIG, August 28th - Septemper 2nd, 2011, Belfast, UK*, 2011.

[11]J. Conway, N. Sirse, S. K. Karkari and M. M. Turner. Using the resonance hairpin probe and pulsed photodetachment technique as a diagnostic for negative ions in oxygen plasma. *Plasma Sources Sci. Technol.*, 19:065002, 2010.

[12]M. Bacal. Photodetachement diagnostic techniques for measuring negative ion densities and temperatures in plasmas. *Rev. Sci. Instrum.*, 71:3981–4006, 2000.

[13]E. C. M. Chen and al. The negative ion states of sulfur hexafluoride. *J. Chem. Phys.*, 88:4711, 1988.

[14]R. A. King, J. M. Galbraith, and H. F. Schaefer. Negative ion thermochemistry: The sulfur fluorides SF_n / SF_n^- (n = 1-7). *J. Phys. Chem.*, 100:6061–6068, 1996.

[15]P. M. Bryant and J. W. Bradley. Optimum circuit design for the detection of laser photodetachment signals. *Plasma Sources Sci. Technol.*, 22:015014, 2012.

[16]S. Kajita and al. Effect of probe surface ablation on laser photodetachment signals. *Contrib. Plasma Phys.*, 44:607–612, 2004.

[17]L.M. Cabalin, J.J. Laserna. Experimental determination of laser induced breakdown thresholds of metals under nanosecond q-switched laser operation. *Spectrochimica Acta Part B*, 53:723–730, 1998.

[18]V. A. Godyak. Electrical and plasma parameters of ICP with high coupling efficiency. *Plasma Sources Sci. Technol.*, 20:025004, 2011.

[19]S. Vacquie, A. Gleizes, and M. Sabsabi. Measurement of the photodetachment cross section of the negative ion of fluorine. *Physical Review A*, 35:1615, 1987.

[20]L. St-Onge, M. Chaker, and J. Margot. Laser-induced photodetachment in high-density low-pressure SF_6 magnetoplasmas. *J. Vac. Sci. Technol. A*, 18:2363, 2000.

[21]A. Aanesland and al. The PEGASES gridded ion-ion thruster performance and predictions. In *33rd International Electric Propulsion Conference, The George Washington University, Washington, D.C, IEPC-2013-259*, 2013.

[22]D. Gerst, M. Cirisany and S. Mazouffre. Investigation of ion-ion plasmas for application in electric thrusters. In *32nd International Electric Propulsion Conference, Wiesbaden, Germany, IEPC-2011-127*, 2011.

[23]St. Kolev, G. J. M. Hagelaar, G. Fubiani and J-P. Boeuf. Physics of a magnetic barrier in low-temperature bounded plasmas: insight from particle-in-cell simulations. *Plasma Sources Sci. Technol.*, 21:025002, 2012.

[24]D. Gerst. *Investigation of Magnetized Radio Frequency Plasma Sources for Electric Space Propulsion*. PhD thesis, Universit d'Orlans, 2013.

[25]J. Bredin. *Dveloppement de diagnostics lectrostatiques pour le filtrage magntique et la formation du plasma ion-ion dans le propulseur PEGASES*. PhD thesis, Ecole Polytechnique, 2013.